Heliyon 5 (2019) e02311

Contents lists available at ScienceDirect

Heliyon

journal homepage: www.heliyon.com

Influence of abrasives and graphite on processing and properties of sintered metallic friction materials

B. Pérez [b], J. Echeberria [a,b,*]

[a] Ceit, Manuel Lardizabal 15, 20018, Donostia/San Sebastian, Spain
[b] Universidad de Navarra, Tecnun, Manuel Lardizabal 13, 20018, Donostia/San Sebastian, Spain

ARTICLE INFO

Keywords:
Materials science

ABSTRACT

In this study, the influence of abrasives (size and morphology) and graphite on the processing and properties of friction materials were investigated. Friction materials based on bronze matrix, graphite as solid lubricant and different abrasives (silica, mullite and zircon) were prepared following two routes. On the one hand, following the traditional P/M technology (pressing-sintering) and on the other hand, using an alternative P/M route, which consists on sintering a powder blend free deposited in a mold and subsequently cold pressing. Sinterability, microstructure and physical-mechanical properties of the processed friction materials have been studied. Tribological and wear tests were carried out on a pin-on-disc system at different loads and sliding speeds using samples of 20 mm in diameter. Results show that the influence of abrasives size is especially relevant in the alternative P/M route, where materials including fine abrasives present unsuitable properties. Graphite also plays an important role on tribological behavior, in this work it has been found that friction materials with 4 wt.% graphite have better tribological properties than those with 2 wt.% graphite, despite having lower density and mechanical resistance.

1. Introduction

Sintered metallic friction materials are a smart choice for heavy-duty applications, like high-speed train brakes or industrial machinery clutches. Currently, there are two main production processes for these systems, namely press sintering (conventional method) and sprinkle sintering method [1]. In the first one, a powder blend is compacted and then, lining green compacts are attached to steel plate and sintered. On the other hand, the sprinkle process is especially useful in the case of clutch discs with large diameter and with friction layer less than 1 mm in thickness. It has the advantage of not requiring any expensive compaction tooling. In this process, the powder blend is free deposited in steel plates and sintered in a conveyor belt furnace with liquid phase. Subsequently, because linings are more porous than in press sintering method, sintered components must be pressed to increase the density and reduce the porosity. Secondary operations are usually required in both processes to achieved smooth surface and close dimensional tolerances [2].

The performance of the brakes and clutches is mainly controlled by the composition and microstructure of the lining material [3, 4]. These materials contain several components and each one plays a different role in friction performance. Principal components are metallic matrix, abrasives and solid lubricants. Generally, sintered metallic friction materials are classified intro two families according to the matrix material, namely copper-based and iron-based materials [5]. Copper-based friction materials are extensively used in friction devices due to their excellent thermal conductivity and wear resistance [3, 6, 7, 8, 9]. Abrasives are usually added to enhance the frictional response of Cu-based materials. The most common abrasives are hard minerals such as silica, alumina, zircon, silicon carbide and numerous oxides of common metals. Abrasives' effectiveness is highly dependent on morphology, size and fracture toughness of the particles. Information about the effect of abrasives on properties of Cu-based friction material is limited. K.H. Cho et al [10] and E. Lee et al. [11] have studied the size effect of zircon and silica particles on friction characteristics of non-metallic brake lining materials. They observed that brake linings with small zircon particles has poor friction stability and large oscillation of the friction coefficient with considerable lining wear, while those with coarse zircon particles showed excellent friction stability and a lower wear rate. Contrary, materials with silica have little difference in the wear rate regardless silica particles size. This is due to the low fracture toughness of silica particles, which leads to size reduction of coarse particles during sliding. The effect of mullite in copper base composite has been studied by V. Jain et al. [2] and they

* Corresponding author.
E-mail address: jjecheberria@ceit.es (J. Echeberria).

https://doi.org/10.1016/j.heliyon.2019.e02311
Received 7 February 2019; Received in revised form 23 July 2019; Accepted 12 August 2019

found that composite which contains mullite and graphite has stable friction coefficient and negligible wear loss. T. Ram Prabhu et al. [12] have reported similar results, materials with large particles of mullite showed better brake performance than those with silica particles due to the greater elastic modulus of mullite.

On the other hand, solid lubricants such as graphite or metal sulphides are required to improve wear resistance [8]. Owing to the lamellar structure and softness of these particles, a solid lubricant film that reduces friction is formed at the contact surface during sliding. Different types of graphite has different properties, for instance graphite in the flake form can improve the lubrication properties, while graphite in the granular form is able to dissipate the heat generated during braking more effectively [13]. However, the addition of graphite to friction material leads to a reduction in mechanical resistance [14]. It is of high importance to find the adequate quantity of graphite to get excellent lubrication properties without reducing friction forces, which are responsible for braking effectiveness.

This work is focused on the influence of particle size and morphology of silica, mullite and zircon, as well as graphite content and type (natural and synthetic) on the processing and properties of copper-based friction materials.

2. Materials and methods

2.1. Samples preparation

Characteristics and morphology of powders used in compositions prepared are shown in Table 1 and Fig. 1, respectively. As metallic matrix, atomized bronze powder with average particle size of 96 μm was used (Fig. 1-a). As solid lubricant two different graphite grades were chosen. One is synthetic (Fig. 1-b) and the other one is natural (Fig. 1-c) with a very different granulometry, as it can be seen in Table 1. Zircon, silica and mullite with different particle size and different morphology were used as abrasives. Table 1 shows their characteristics and Figure 1 (d-i) presents their morphology and size. Flour zircon, mullite and silica 2 were sieved using a mesh of 50 μm to remove the finest fraction, which is the responsible for a poor sintering. Table 1 includes the average particle size of these powders before and after sieving. It can be seen how median particle size of zircon and mullite flour increases considerably.

To study the influence of abrasives size on processing and properties of friction materials, four different compositions divided in two groups were prepared with the relative content of each element as shown in Table 2. On the one hand, compositions with coarse abrasives (sand-S) and on the other hand, ones with fine abrasives (flour-F). To analyze the influence of graphite, the weight % was increased from 2 to 4 in group S. Not only the influence of the amount of graphite were studied, but also the influence of the type of graphite, i.e. synthetic or natural in composition S4 and S4N respectively. In composites S2, S4, S4N and F2 zircon, silica and mullite were used, while S2Z and F2Z contain only zircon as abrasive.

Table 1
Characteristics of powders used in compositions.

Powder	Supplier	Ap. Density (g/cm^3)	Av. particle size (μm)	
			As received	Sieved (50μm)
Bronze	Ames	2.7	96	-
Zircon sand	CMMP	4.6	140	-
Zircon flour	CMMP	4.6	9	47
Silica flour 1	Sibelco Minerals	-	39	-
Silica flour 2	Amberger Kaolinwerke	-	23	78
Mullite sand	Dupré Minerals	-	270	-
Mullite flour	Dupré Minerals	-	43	89
Graphite synth.	Imerys	0.3	21	-
Graphite nat.	Imerys	-	300	-

Bronze, silica, mullite, zircon and graphite powders were blended in the required proportions (Table 2) in a Turbula mixer for 1 h. Steel balls of 6 mm in diameter were used as grinding media, with a ratio 1:9 with respect to the powder. After the blending process, specimens with different geometry were prepared following two routes:

- R1: Conventional P/M route (press-sinter process). Cylindrical pins of 20 mm in diameter and 10 mm in height for wear tests and bars of 25 × 7 × 5 mm for Three Point Bending test were compacted at 400 MPa using a uniaxial compaction press. Green specimens were sintered in a MRF furnace (Materials Research Furnaces Inc.) at 800–900 °C in reductive atmosphere (Ar/H_2) for 1 h.
- R2: Alternative P/M route (similar to sprinkle process). Blended powders were free deposited in molds of 25 and 40 mm in diameter with a powder height of 15 and 8 mm respectively. Subsequently, the powders in molds were sintered at 850–925 °C in reductive atmosphere for 1 h in the same furnace used in R1. After sintering, specimens were separated from molds and cold pressed at 150–250 MPa to reduce the porosity up to 20%, similar to that obtained in R1. Finally, samples were machined to adapt their dimensions to that required for wear tests (20 mm in diameter and 10 mm in height) and for bending tests (bars of 25 × 7 × 5 mm).

Preliminary tests of dilatometry and Differential Scanning Calorimetry (DSC) were carried out in S2 composite in order to determine the optimum sintering temperature for both routes (R1 and R2). Dilatometry tests were performed in a horizontal Netzch 402/7 dilatometer using cylindrical specimens of 6 mm in diameter compacted by uniaxial cold pressing at 400 MPa. The temperatures range studied was 800–900 °C with a heating and cooling rate of 10 °C/min and a dwell time of 1 h. Reductive atmosphere of 90%N_2:10%H_2 was used. On the other hand, DSC tests were carried out using a DSC/TGA Setaram Setsys Evolution 16/18 equipment, up to 1100 °C with a heating rate of 10 °C/min and a cooling rate of 20 °C/min. Nitrogen was used as protective atmosphere against oxidation.

2.2. Characterisation methods

Apparent density and porosity of samples were determined by Archimedes' water immersion principle. Microstructure of the different compositions were analysed using a Philips XL30CP Scanning Electron Microscope (SEM) with EDS by EDAX and a Dual Beam Quanta 3D FEG with EDS Oxford INCA 450.

Mechanical properties were determined by three points bending test in accordance with ISO 3327. TRS (Transverse Rupture Strength) value for each composite was reported based on average several samples test.

Tribological performance of the composites was studied as function of applied normal load (N) and sliding speed using an adapted pin-on-disc system which was designed, fabricated and started up in CEIT [15, 16]. All tests were carried out at room temperature at applied normal loads of 0.8 and 1 MPa and sliding speeds of 4.5 and 7.1 m/s. Cylindrical samples of 20 mm in diameter were used as pins and steel F114 as counter disc. Before and after each test, pins were weighed to determine the amount of wear loss. Tangential frictional load (F) were recorded along 10000 m of sliding and friction coefficient (μ) was calculated using (1).

$$\mu = F/N \quad (1)$$

3. Results and discussion

3.1. Sinterability study

Results of calorimetry and dilatometry tests at 800, 850 and 900 °C for S2 composition are shown in Fig. 2. Heat flow curve as function of

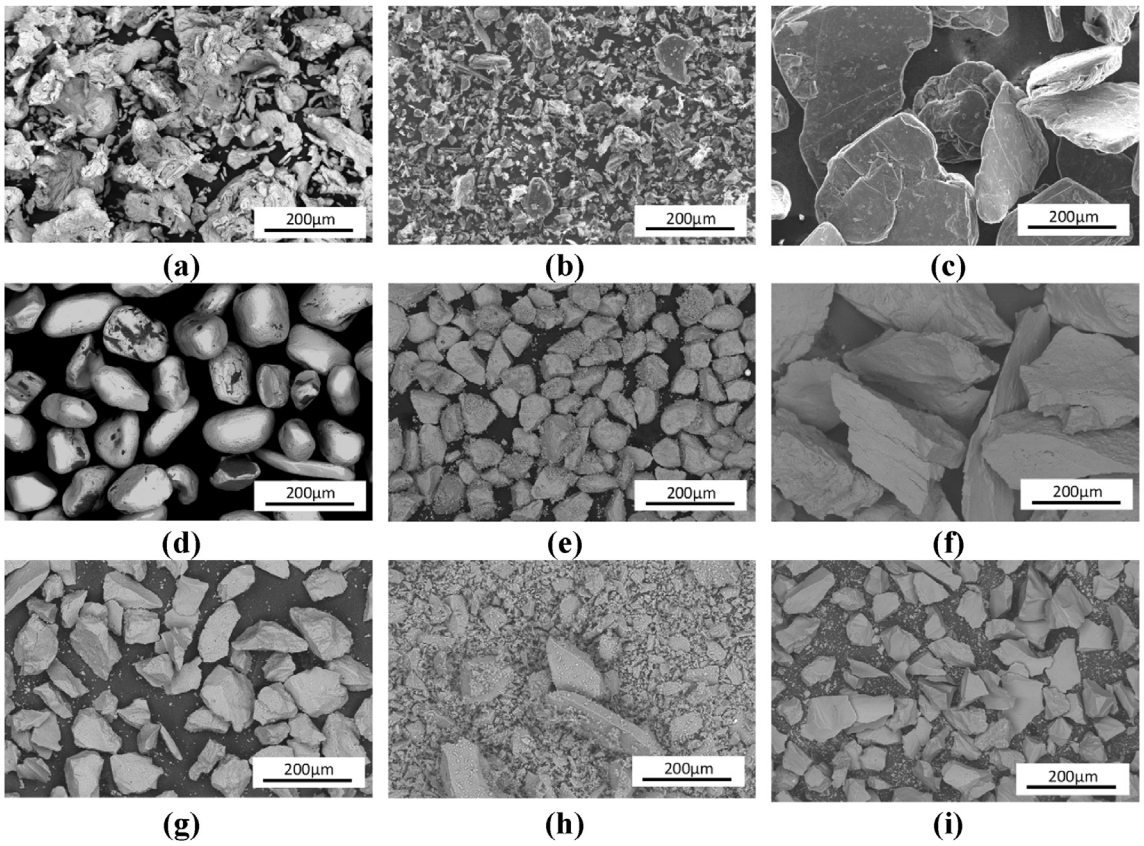

Fig. 1. SEM images of (a) atomized bronze, (b) synthetic graphite, (c) natural graphite, (d) $ZrSiO_4$ sand, (e) sieved $ZrSiO_4$ flour, (f) mullite sand, (g) sieved mullite flour, (h) SiO_2 flour 1 and (i) SiO_2 flour 2.

Table 2
Relative content of raw materials in friction materials studied.

	Raw material	Type	%wt						
			S2	SZ2	S4	SZ4	S4N	F2	FZ2
Metal matrix	Bronze	Cu–Sn–Zn	87	87	85	85	85	87	87
Abrasives	Zircon	Flour	-	-	-	-	-	7	11
		Sand	7	11	7	11	7	-	-
	Silica	Flour 1	2	-	2	-	2	-	-
		Flour 2	-	-	-	-	-	2	-
	Mullite	Flour	-	-	-	-	-	2	-
		Sand	2	-	2	-	2	-	-
Lubricant	Graphite	Synth.	2	2	4	4	-	2	2
		Nat. L	-	-	-	-	4	-	-

temperature is represented in Fig. 2 (a). An endothermic peak can be observed (between 850 and 1020 °C) related to the melting of bronze, with a solidus temperature (T_S) of 850 °C and a liquidus temperature (T_L) of 1020 °C. An exothermic peak can also be seen, corresponding to the solidification of the liquid during cooling. T_L and T_S during cooling are 1000 and 900 °C, respectively.

As observed in Fig. 2, the dilatometry analyses can be correlated to that pointed out by DSC. According to the dilatometry curves, shrinkage by solid state sintering starts at 585 °C. The presence of both graphite and abrasives limits this linear shrinkage only up to a 1%. This behaviour is shown in Fig. 2 (b), which correspond to the dilatometry-sintering test carried out at 800 °C, before the formation of the liquid. On the other hand, in the sintering tests performed at 850 °C, that is the bronze solidus temperature, T_S (as determined by DSC), an additional shrinkage takes place, characterised by a slope change of the curve, that is promoted by the presence of the liquid. Comparing Figure 2 (c) and (d), an increase of the temperature up to 900 °C means an increase of the amount of liquid and therefore, the shrinkage due to liquid phase sintering increases during both heating step and dwell time (60 min). In contrast, at 850 °C, due to the presence of a very low amount of the liquid phase, almost no additional shrinkage is produced during dwell time.

Therefore, considering this shrinkage behaviour, liquid phase sintering is required to achieve a good densification during sintering, and the final density will depend on the amount of liquid formed as a function of the temperature. However, an excess of liquid could be detrimental during sintering, as it is observed in the dilatometry test carried out at 900 °C (Fig. 2 d). Due to the poor wettability of the bronze liquid with graphite particles and abrasives and its reduction of the viscosity with the temperature, an excess of liquid can be promote its exudation (part of liquid flows out the sample), or the swelling of the component [17]. The last effect has been observed in the dilatometry test performed at 900 °C during the beginning of cooling.

From these results, and taking into account the particular processing conditions of Route 2, sintering temperature was stablished in the range

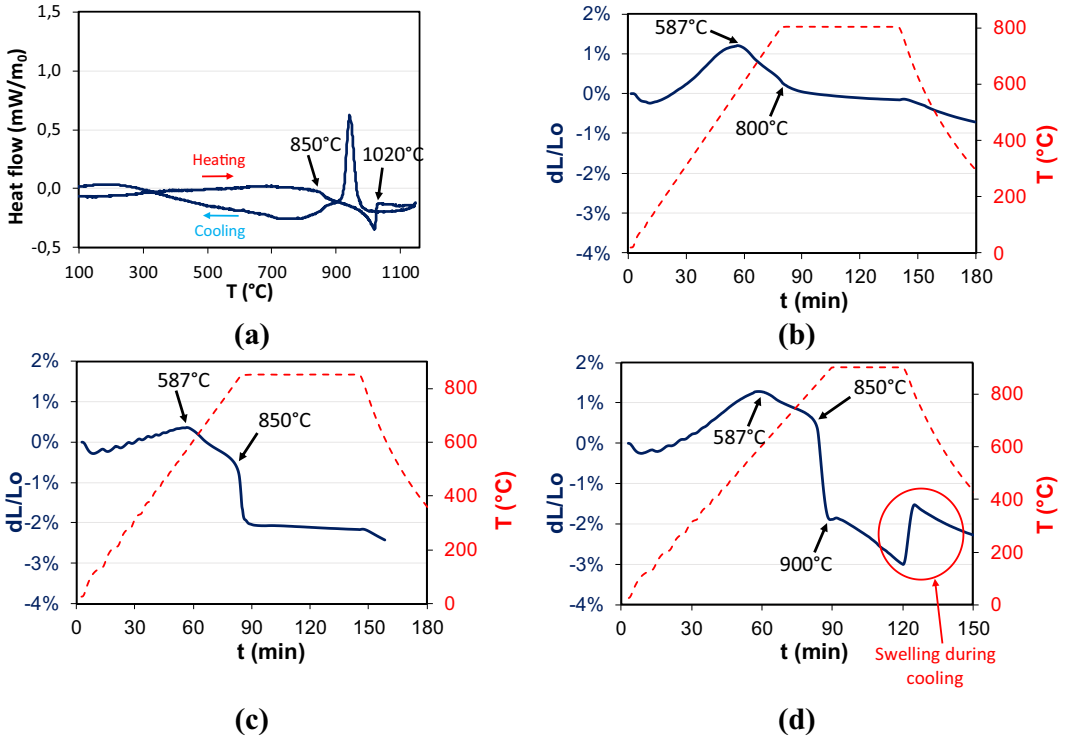

Fig. 2. (a) DSC curve of S2 material, (b) dilatometry up to 800 °C, (c) 850 °C and (d) 900 °C curves for S2 material processing by route 1.

of 850–900 °C. Nevertheless, sintering behavior of the different compositions is strongly dependent on processing conditions used in each route. Therefore, it is of high importance to perform sintering tests to samples processed following both routes and determine the appropriate sintering conditions for each one.

First sintering tests on green preforms were carried out with S2 composition (the same used for DSC and dilatometry experiments) processed according to Route 1. The results obtained are shown in Table 3. In accordance with results obtained in dilatometry tests (Figure 2 b-d), shrinkage of sample does not take place until the appearance of liquid phase at 850 °C. However, at 900 °C, the quantity of liquid seems to be excessive, since part of it exudes due to its low wettability with abrasives and graphite particles.

As observed in Table 3, mechanical resistance (TRS) increases with sintering temperature. This suggests that, although before bronze T_S (850 °C) density and porosity values are similar to that of green sample, the process of particles bonding takes place, providing sample with strength. As expected, the highest mechanical resistance (TRS) is obtained at 850 °C, when liquid phase begins to appear. It enhances particles bonding and activates the sintering process getting a more strengthened matrix structure.

On the other hand, samples processed by Route 2 (loosed powder sintering) were only sintered at temperature above bronze solidus temperature due to the requirement of liquid phase sintering, especially in this processing route. Specimens of S2 sintered at different temperatures are shown in Fig. 3.

Table 3
Density, porosity and TRS of S2 sample processing by Route 1 as function of sintering temperature.

	Green	Sintering Temperature (°C)			
		800	825	850	900
Density (g/cm^3)	5.88	5.81	5.82	6.03	Exudation of liquid
Porosity (%)	19	20	20	18	
TRS (MPa)	-	79	106	148	

Contrary to Route 1, S2 powder blend sintered at 850 °C does not get enough consistency; this leads to think that liquid amount formed at this temperature is not enough to activate the densification process in this route. Therefore, there is a big difference between sintering a green compact pressed at high pressure (400 MPa) and a mold filled with loose powder. In order to enhance the densification promoted by the presence of more amount of liquid and with lower viscosity, temperatures up to 925 °C were tested.

As observed in Fig. 3, exudation takes place in R2 at higher temperature than in R1, 925 °C. Lower temperatures between 850 and 900 °C seems to be the adequate sintering temperature in this route. Sample sintered at 875 °C as well as that sintered at 900 °C have good aspect and densification, without the presence of any solidified liquid phase on the surface of the compact.

Values of apparent density and porosity of S2 sintered at 875 and 900 °C are shown in Table 4. Densification is quite similar for both sintering temperatures, it has been achieved a 70% of theoretical density; however, lower density is obtained at 900 °C. Therefore, 875 °C has been considered enough temperature to consolidate this material following Route 2. As expected, these values are lower than that obtained in Route 1, but they are acceptable considering that these as-sintered samples need a cold pressing step to increase the density and reduce porosity.

These results are consistent with dilatometry tests and confirm that liquid phase sintering plays an important role in the densification of these materials in both processing routes. Moreover, samples sintered by Route 2 require higher volume fraction of liquid phase to densify, because the apparent density of loose powder (2.73 g/cm^3) is much lower than green density of compacts (5.88 g/cm^3). Consequently, densification during sintering is more difficult in R2, as powder particles in the mold are more separated from each other than in compacted samples. Considering these results, sintering temperature of S2 was established at 850 °C for Route 1 and 875 °C for Route 2.

3.2. *Influence of abrasives*

In order to verify if 875 °C is also a suitable sintering temperature for

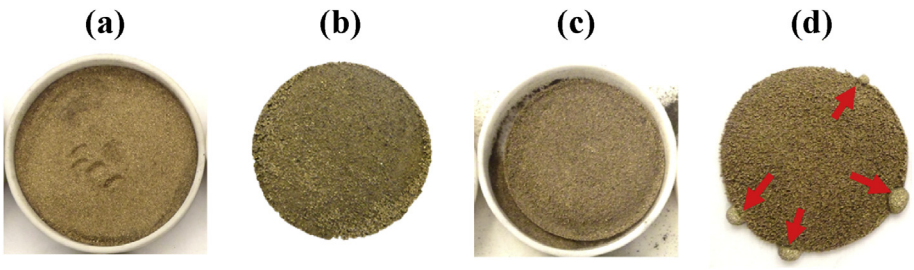

Fig. 3. S2 specimens sintered at (a) 850 °C, (b) 875 °C, (c) 900 °C and (d) 925 °C following Route 2 before cold pressing stage. Liquid exuded from the compact is marked with red arrows.

Table 4
Density and porosity of samples S2 after sintering at 875 °C and 900 °C following Route 2.

	875 °C	900 °C
Sintered Density (g/cm^3)	5.33	5.27
Porosity (%)	26	28

composition with fine abrasives (F2), sintering tests between 875 and 900 °C was carried out with F2 sample processed by Route 2. Fig. 4 shows the aspect of F2 samples after sintering process. As observed, part of the liquid has exuded from the compact. at 900 °C. This effect was not observed at this temperature in S2 material (Fig. 3). This difference is related to the fact that fine abrasives have more specific surface area and, consequently liquid is more prone to exude. Therefore, it can be stated that particle size of abrasives is the main factor that influence the densification behavior of these materials processed by Route 2.

On the other hand, sample sintered at 875 °C, in the same way that S2, presents good aspect and acceptable densification (density of 4.63 g/cm^3 – 35% porosity), although, as expected, it is lower than that of S2, which presents a density of 5.33 g/cm^3 and 26% of porosity. Considering this behavior, sintering temperature for F2 in Route 2 was also stablished at 875 °C.

Once the sintering conditions for both compositions and processing routes were stablished (R1: 850 °C and R2: 875 °C), the influence of granulometry and type of abrasives on processing and properties of friction materials were analyzed. For that, composites S2 and SZ2 (coarse abrasives) were compared with F2 and FZ2 (fine abrasives), processed following both routes. In R2, sintered samples were subsequently cold pressed to enhance the density and reduce the porosity to the target value (20%).

3.2.1. *Physical and mechanical properties*

Fig. 5 compares the apparent density and porosity of composites processed by the two routes. For R2, values of sintered density and porosity before and after the subsequent cold pressing step are included.

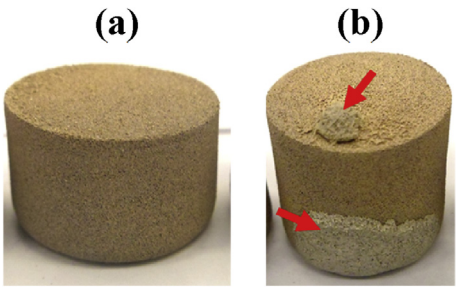

Fig. 4. F2 specimens sintered at (a) 875 and (b) 900 °C following Route 2 before cold pressing stage. Liquid exuded from the compact is marked with red arrows.

As observed in Fig. 5, fine abrasives (series F), due to their higher surface area, make sintering more difficult than coarse ones (series S), getting lower densities and higher porosities after the sintering stage. This is more significant in R2, since the restriction of higher surface area fine abrasives to the densification and boundary of bronze particles is greater in this processing route, where green preform are loose powder in mold. On the other hand, when mullite and silica are replaced by zircon in compositions SZ2 and FZ2, sintering is improved in both processing routes, since higher densification, compared to S2 and F2, respectively, is achieved.

A cold pressing stage after sintering is needed in Route 2 to reduce porosity up to a similar value than that achieved in Route 1 (~20% porosity). The pressure required to apply in this step is highly dependent on sample's porosity (%) after sintering. In Table 5, applied pressure, porosity after sintering and after cold pressing stage are presented. As observed, due to the higher porosity of as-sintered materials with fine abrasives (F2 and FZ2), higher pressure is needed to get the same porosity than S2 and SZ2 (with coarse abrasives).

Microstructure of S2 and F2 processed by R1 and R2 after sintering stage and after cold pressing are shown in Fig. 6 (a), (b) and (c), respectively. Firstly, comparing microstructure of samples after the sintering step in both routes (Figure 6 a-b), larger bronze metal matrix's grain size is obtained in R2 due to higher sintering temperature (875 °C vs. 850 °C) used in this processing route, and promoted by the presence of more amount of liquid phase during sintering. On the other hand, poorer densification during sintering is achieved in samples processing by R2, leading to more porosity in bronze matrix and in the interface matrix-abrasives, as it is observed in Fig. 6 (b).

Regarding abrasives' particle size, micrographs shown in Fig. 6 confirm the fact that fine abrasives (series F) make sintering more difficult than coarse ones (series S). Due to that, when fine abrasives are used (F2), bronze matrix does not present a continuous structure as it does when coarse ones are used. This is more evident in Route 2 (Fig. 6-b) where the sinterability is poorer. The larger specific surface area of fine abrasives leads to an ineffective sintering process and prevents grain growth. Consequently, higher grain size of bronze is observed in material with coarse abrasives (S2).

The difference in volume of porosity between R1 and R2 after sintering stage is reduced with cold pressing process. Fig. 6 (c) shows the microstructure of samples S2 and F2 processed by R2 after cold pressing step. Although porosity is reduced up to similar values to that obtained in R1 (Fig. 6-a), matrix seems to be less continuous in samples processing by Route 2 (Fig. 6-c), especially in F2 where bronze particles are in contact due to reduction of the porosity but not well bonded. This effect is clearer distinguished at higher magnifications, as observed in Fig. 7. Another difference between the microstructure obtained by both routes is that grain structure has been deformed along the perpendicular direction of compaction during cold pressing step in R2. This fact is more evident in F2 because it required higher pressure due to its higher porosity before this step.

Fig. 8 shows the microstructure of SZ2 and FZ2 processed by Route 1. Comparing them with S2 and F2 (Fig. 6-a), it is observed that, as

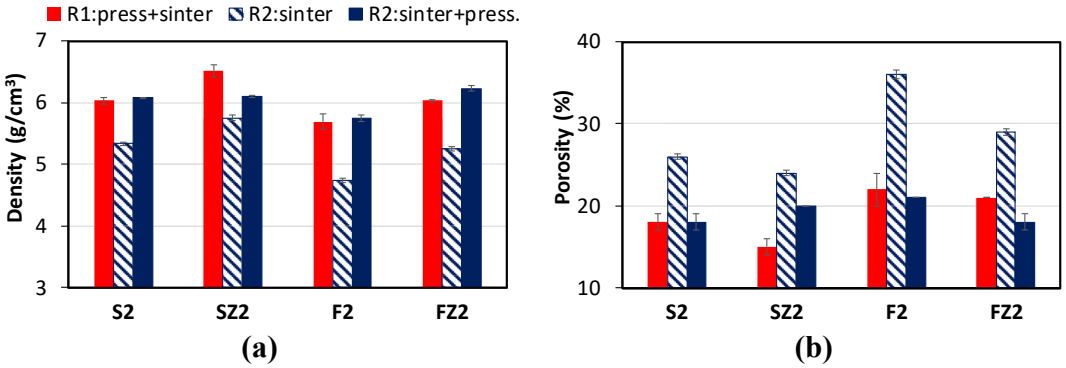

Fig. 5. (a) Density and (b) porosity as function of manufacturing route and abrasives granulometry.

Table 5
Pressure applied in cold pressing stage in Route 2 as function of abrasives size and initial porosity.

	Pressure Pressing (MPa)	Porosity after sintering (%)	Porosity after cold pressing (%)
S2	160	26	18
SZ2	130	24	20
F2	230	36	21
FZ2	190	29	18

mentioned before, better densification is obtained when only zircon is used as abrasive. This improvement seems to be related with round and smooth morphology of zircon, comparing with sharp and angular particles of mullite and silica (Fig. 1), which makes easier having more contact surfaces among bronze particles, which results in less porosity and greater consolidation of metal matrix, in addition to better interface matrix/abrasives.

Finally, Table 6 presents the TRS values and % porosity of compositions processed following R1 and R2 (sintering + cold pressing). It is observed that TRS is higher for specimens developed by R2 in all composition studied, although apparent density and porosity obtained in

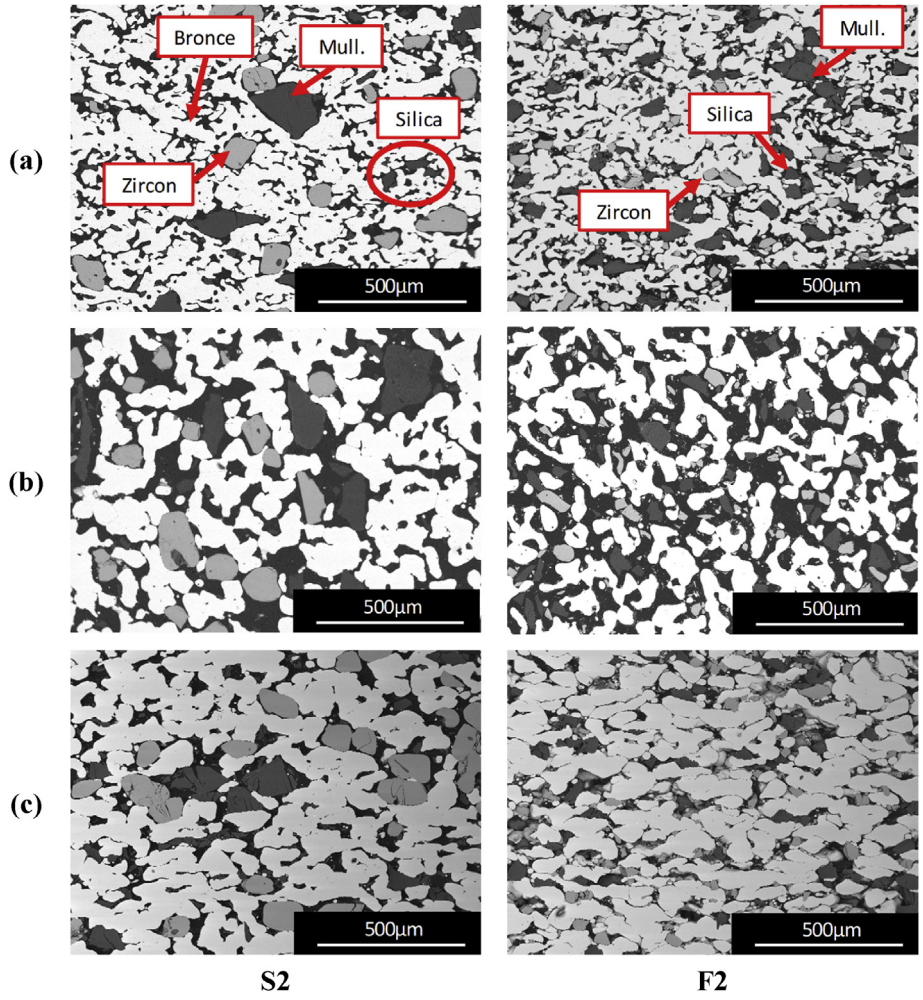

Fig. 6. Microstructure of S2 and F2 materials processing by route 1 (a) and route 2 as sintered (b) and after cold pressing stage (c).

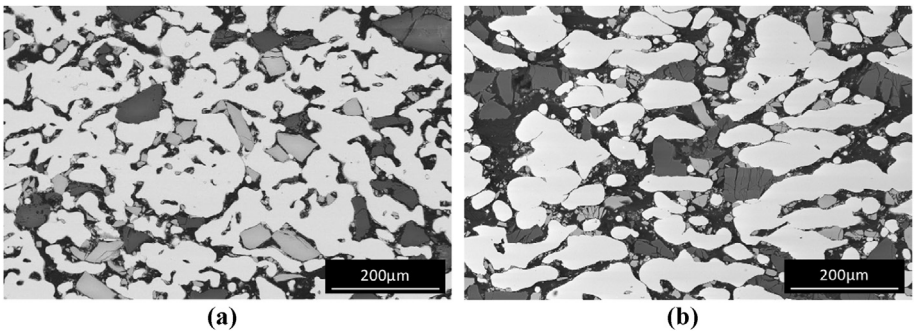

Fig. 7. Materials F2 processing by (a) Route1 and (b) Route 2 after cold pressing stage.

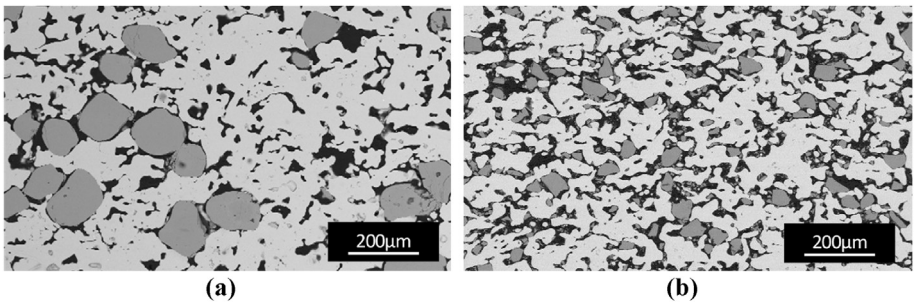

Fig. 8. Microstructure of SZ2 (a) and FZ2 (b) sintered at 850 °C (route 1).

Table 6
TRS (MPa) values and % porosity (%P) of materials studied as function of manufacturing route.

	S2		SZ2		F2		FZ2	
	R1	R2	R1	R2	R1	R2	R1	R2
%P	18	18	15	20	22	21	21	18
TRS	148	204	197	200	108	137	128	161

both routes are similar. Therefore, the higher mechanical strength of specimens processed by R2 may be related to the strain hardening of the bulk material caused by the cold pressing step after sintering [2]. In the case of SZ2, almost no difference in TRS is observed between both processing routes. This may be because, on the one hand, the pressure applied by cold pressing in this material is relatively low and consequently, lower effect of strain hardening is produced, and on the other hand, because of the higher porosity % in the specimens produced by R2, 20% versus 15% obtained in R1.

Regarding the influence of the abrasives' type and granulometry, it is clearer observed in Fig. 9. Higher densification achieved in samples with only zircon as abrasive (SZ2 and FZ2) leads to achieve higher TRS values.

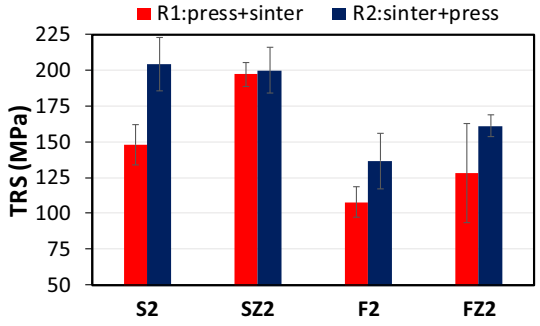

Fig. 9. TRS as function of manufacturing route and abrasives' granulometry.

Besides, it can be stated that abrasives size has a great influence in mechanical resistance of materials since TRS values decrease significantly when fine abrasives are used (F2 and FZ2). This is related to the lack of metal matrix consolidation during sintering of samples F2 and FZ2 observed by SEM (Fig. 7 b).

3.2.2. *Tribological behavior*

Friction tests were carried out on samples of both series and processed following both routes. From these tests, friction coefficient (μ) and wear resistance, measured as mass loss, were obtained. The average friction coefficient (μ) of the different materials processed by Route 1 and Route 2 as a function of sliding speed and applied load are shown in Table 7. F2 processed by R2 was not tested at all conditions because it had severe wear under softer conditions, and FZ2 processed by Route 2 was not tested due to its high wear when processed by Route 1.

As shown in Table 7, friction coefficient varies in a range of 0.31–0.45 decreasing when sliding speed increases. This behavior, related to the "fade phenomena" [10], has been associated in other studies to the interface temperature during sliding [14, 18, 19, 20]. Temperature in contact interface raises when sliding speed increases and this lead to the oxidation of the friction film, which acts as lubricant film and prevent the contact between both surfaces decreasing μ and wear. Worn surfaces of S2 and F2 materials were analyzed by GIXRD in [21] and more copper and iron oxides were found in materials tested at higher sliding speed (7.1 m/s), which confirms the higher temperature achieved at higher sliding speed and the oxidized protective film formed in the materials surfaces. On the other hand, in [22], the reduction in μ when sliding speed increases has been attributed to the fact that granulated debris, formed at lower sliding speed, becomes rather dense having a role of lubrication. With respect to normal pressure, there are not significant changes in μ when pressure increases. This behavior has also been found in other studies [18, 23].

Additionally, as observed in Table 7, μ of these materials depends strongly on the processing route used. Values suggest that samples processed by Route 1 have a superior friction performance, specially samples with fines abrasives, since when they were processed by Route 2, they could not be tested due to their severe wear.

Table 7
Average friction coefficient (μ) of composites developed following Route 1 (R1) and Route 2 (R2).

	ROUTE 1				ROUTE 2			
	4.5 m/s		7.1 m/s		4.5 m/s		7.1 m/s	
	0.8MPa	1MPa	0.8MPa	1MPa	0.8MPa	1MPa	0.8MPa	1MPa
S2	0.40	0.42	0.32	0.34	0.41	0.45	0.36	0.36
SZ2	0.38	0.38	0.33	0.31	0.44	0.42	0.34	0.35
F2	0.41	0.42	0.34	0.36	0.48*	-	-	-
FZ2	0.43*	0.48*	-	-	-	-	-	-

* Incomplete test. (-) Test were not carried out.

Regarding the nature/morphology of abrasives and comparing S2 and SZ2 (coarse abrasives) processed by R1, it can be pointed out that μ is more stable when using only zircon as abrasive (SZ2). This could be because SZ2 presents higher densification than S2 that lead to a smooth friction surface. However, comparing F2 and FZ2, it is observed that in this series (fine abrasives) using only zircon (FZ2) is detrimental for friction performance of the material, although higher densification and TRS are obtained in FZ2. This is related to the fact that flour zircon used in FZ2 is the finest abrasive powder used in this work (D_{10}: 1μm), while the finest particles (D_{10}) of mullite and silica used in F2 are of 50 and 36 μm, respectively. Due to the weaker bond of fine particles with matrix, the finer abrasives are, the higher is the probability of their removal from matrix. Some of these removed abrasive particles might be trapped in the interface acting as a third body and increasing the wear of material. Therefore, not only the nature/morphology of the abrasive influences the friction performance of these materials, but also their granulometry.

With respect to abrasives' granulometry, depending on the difference of particle size, it has more or less influence on the tribological behavior. In the case of F2 and S2 processed by R1, similar friction behavior has been found, despite of less densification of F2. Nevertheless, very different behavior is observed between SZ2 and FZ2 (Table 7). As mention before, FZ2 could not be tested under any conditions due to severe wear of samples related to the much finer zircon used in FZ2 than in SZ2.

Turning now to friction performance of materials processing by Route 2 (Table 7), materials with coarse abrasives (S2 and SZ2) show similar values of friction coefficient and both materials have slightly higher μ values than that of samples produced by Route 1. These differences could be related to the strained surface with the subsequent residual stresses generated by the cold pressing step used in R2, which promote higher friction forces [2].

Abrasives' granulometry has even more influence in the tribological behavior of materials processed by R2. Densification achieved after sintering of materials with fine abrasives (F2 and FZ2) is very low and, although cold pressing step increases density, bonding of bronze particles is not enough, as observed in Figure 6 (b,c). The lack of effective metallic

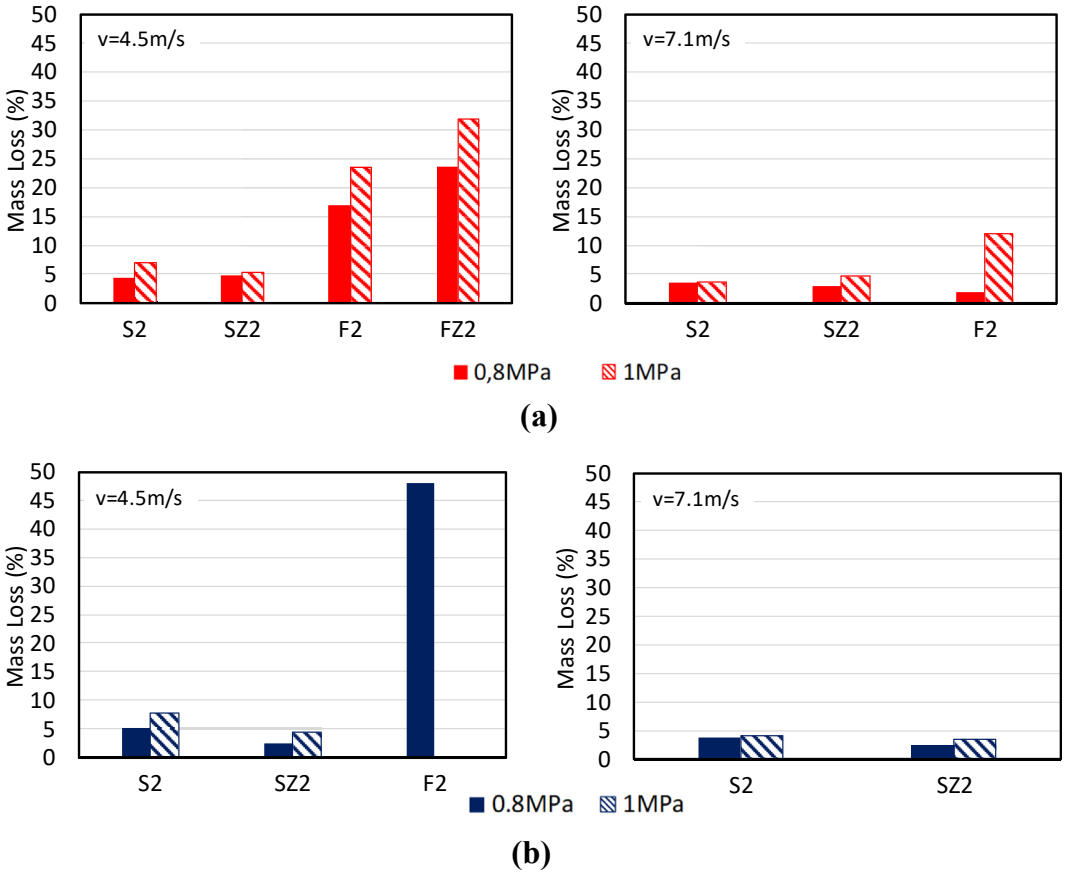

Fig. 10. Effect of abrasives' granulometry and processing in wear loss of materials prepared by Route 1 (a) and Route 2 (b).

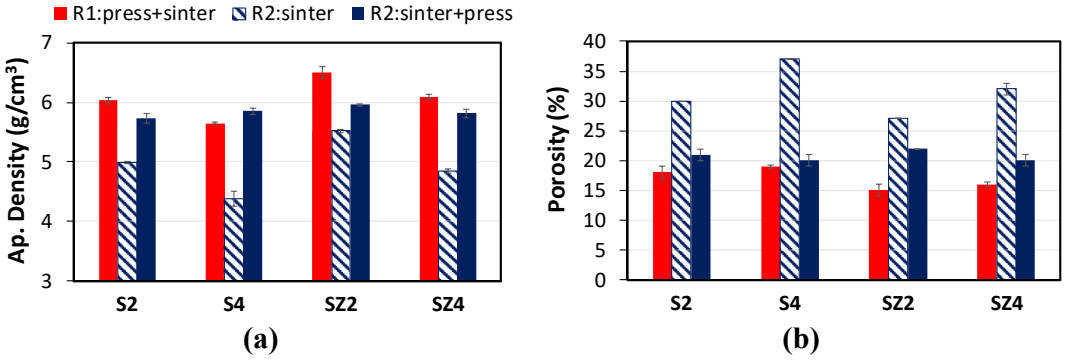

Fig. 11. Influence of %weight of graphite in apparent density (a) and porosity (b) of samples with three abrasives (S) and only zircon (SZ).

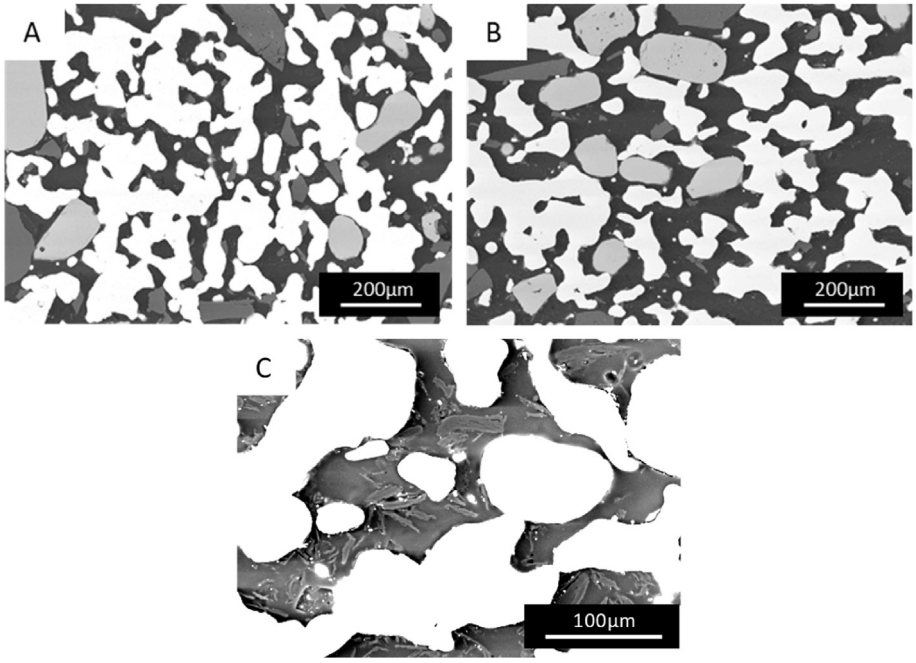

Fig. 12. Microestructure of S2 (A) and S4 (B–C) as sintered by Route 2. (C) has high contrast to visualize graphite particles in samples S4.

Table 8
Pressure applied in cold pressing stage in Route 2 as function of graphite %wt.

	Height reduction (mm)	Pressure Pressing (MPa)	Porosity after sintering (%)	Porosity after cold pressing (%)
S2	4.0	160	30 ± 0	21 ± 1
S4	6.1	160	37 ± 0	20 ± 1
SZ2	3.1	133	27 ± 0	22 ± 0
SZ4	4.7	140	33 ± 1	20 ± 1

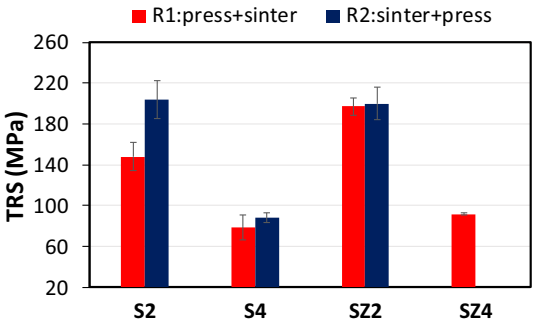

Fig. 13. TRS as function of %graphite.

matrix structure, in addition to the fact that fine abrasives are weaker held in metallic matrix, makes easier to pull out abrasive particle during sliding leading to great mass losses.

The analysis of the wear values (Fig. 10), measured as mass loss (%) during friction test, also reveals higher differences between the tribological behavior of materials processing by the two routes. Regarding the parameters of the wear tests (velocity and pressure), it can be pointed out that when sliding speed increase, wear loss decreases for both processing routes. As mentioned before, this may be related to the increase of the interface temperature with the increase of sliding speed. Consequently, loose particles of debris, generated during sliding, are deformed along sliding direction producing an smooth oxidized layer that cover worn surface of composite and acts as lubricant decreasing both μ and wear [14]. Regarding pressure applied, as expected, the wear loss slightly increases in all specimens when pressure raises, owing to higher contact area between composite and counter-disc. Materials with fine abrasives (F2 and FZ2) are more sensitive to pressure's effect.

Materials with coarse abrasives (S2 and SZ2) processed by both routes exhibit similar wear resistance, despite composition with only zircon as abrasive (SZ2) has higher densification and TRS.

Comparing the values of wear loss measured in both series (S and F)

Table 9
Average friction coefficient (μ) of composites processed following route 2 as function of %weight of graphite.

	ROUTE 2			
	4.5 m/s		7.1 m/s	
	0.8MPa	1MPa	0.8MPa	1MPa
S2	0.41	0.45	0.36	0.36
S4	0.47	0.44	0.43	0.43
SZ2	0.44	0.42	0.34	0.35
SZ4	0.43	0.47	0.41	0.38

included in Fig. 10, it is observed that composites with coarse abrasives (S2 and SZ2) present good behavior with mass losses lower than 7% under all test conditions. However, composites with fine abrasives (F2 and FZ2) show severe wear that, as mentioned before, is owing to the weakly bond between fine abrasives with the metallic matrix.

The deterioration of the wear resistance when fine abrasives are used is more evident in materials processed by Route 2. Once again, it is related to the lack of cohesion in metal matrix of specimens produced by this route, which makes easier the fact that abrasives were pulled out and trapped between friction surfaces. Hence, third body abrasion takes place producing large amount of wear in samples surface [10, 11].

3.3. Influence of graphite

The study the effect of graphite on the processing and properties of friction material has been divided in two parts. In the first one, the influence of weight % of graphite (from 2 to 4%) is analysed in compositions with coarse abrasives (S and SZ). On the other hand, the second part is focused on the influence of graphite's type, i.e. natural or synthetic, in processing and properties of friction materials.

3.3.1. As function of weight % of graphite

In order to study the effect of quantity of graphite on properties of friction materials studied, composition S2, SZ2 (2% G) and S4, SZ4 (4% G) are compared. The apparent density and porosity of samples processed by both routes are represented in Fig. 11.

As expected, the apparent density obtained is lower when graphite % raises. This is because a combination of different aspects, graphite's lower specific density, low wettability of graphite particles by bronze matrix [2] and the graphite's spring-back which takes place during compaction and sintering in Route 1. Besides, related to this lower density, the porosity is slightly higher in material with higher graphite %.

The same tendency has been found in the densification behavior for both processing routes. However, the increase of porosity when graphite content raises (S2–S4; SZ2-SZ4) is more noticeable in samples processed by Route 2. In this case, the porosity is increased by 6–7% when increasing the content of graphite in the base material by 2%, whereas in Route 1 the increase of porosity is only 1%. Once again, any change in the composition or nature/morphology of the friction material's constituents has a great relevance in materials processed through the Route 2.

In the same way that, as it happened in materials with 2% graphite (S2 and SZ2), in those containing 4% (S4 and SZ4), a better densification during sintering is obtained when zircon is used as the only abrasive (SZ4).

Fig. 12 shows the microstructure of samples S2 and S4 processing by Route 2 after the sintering stage. As observed in micrographs, as graphite content increases, the porosity also increases. Large pores are also distinguished in Fig. 12-C, they are mainly located around graphite particles, which evidence the low wettability of graphite and bronze.

Table 8 shows the pressure that is required to apply in the cold pressing stage after sintering of the samples produced by Route 2. Despite the greater initial sintered porosity obtained in the materials with higher % of graphite, almost no difference of pressure required to get the porosity target (20%) has been determined. However, as observed in Table 8, the height reduction of S4 sample was higher than that of S2 applying the same pressure. This suggests that graphite enhances the compressibility of these materials.

Regarding the mechanical resistance, TRS values of samples with both graphite content processed by both routes are represented in Fig. 13. As expected, the higher graphite content, the lower the TRS. Taking into account the low graphite strength [2], the decline in resistance is directly related to the increase of the amount of graphite and, in Route 1, to the slight increase of porosity.

To study the graphite's influence on the tribology behavior of these materials, only materials processed through Route 2 were tested. The average friction coefficient values and mass loss charts of the different materials processed by R2 are included in Table 9 and Fig. 14, respectively.

In general, friction coefficient increases with % graphite, which is contrary to what is reported [3, 24, 25, 26, 27]. In this case, it can be considered that specimens with 4% graphite content have more plastic deformation degree after cold pressing stage in R2. Despite the pressure applied is very similar to that applied in materials with 2% graphite, the thickness reduction is higher in materials with 4% of graphite, since the previous sintered porosity was greater. Because of that, residual stresses may be higher which can lead to higher friction force [2] and hence an increase in friction coefficient.

The μ values shown in Table 9 indicate that the fade resistance is improved increasing graphite wt. % from 2 to 4 (S4 and S4Z), since μ decrease with sliding speed is significantly lower (specially for S4) than

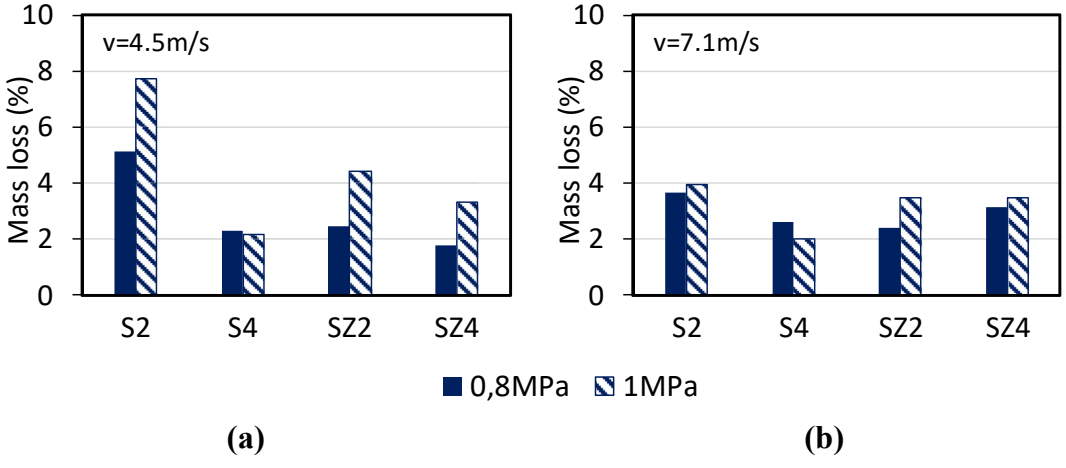

Fig. 14. Effect of graphite in wear of composites processed by Route 2 tested a sliding speed of (a) 4.5 m/s and (b) 7.1 m/s.

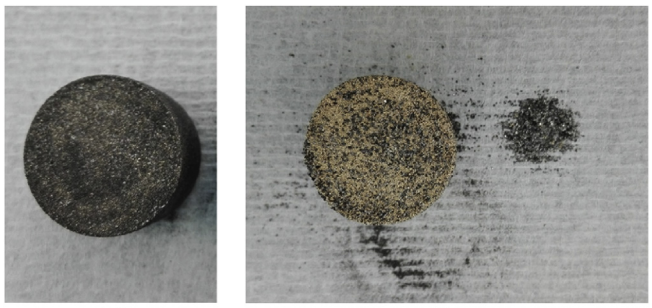

Fig. 15. Aspect of samples after sintering stage in Route 2. (a) S4 with synthetic graphite and (b) S4N with natural graphite.

Table 10
Apparent density, porosity and TRS values as function of graphite's type and processing route.

	ROUTE 1		ROUTE 2 (after sintering)	
	S4	S4N	S4	S4N
Green density (g/cm^3)	5.68	5.60	-	-
Ap. Density (g/cm^3)	5.56	5.84	4.38	4.14
Porosity (%)	19	16	37	40
TRS (MPa)	79 ± 12	140 ± 11	-	-

in composition with 2% graphite (S2 and SZ2).

Not only friction behavior is improved when graphite content increases, but also mass loss is lower for compositions with 4% graphite (Fig. 14). This fact is more significant for low sliding speed (4.5 m/s) since wear loss decreases from 8 to 2% in composition S2–S4 respectively for pressure applied of 1 MPa. This behavior leads to suppose that 2% graphite is not enough to achieve a good lubrication in composites studied; to get an acceptable friction and wear resistance at least 4% graphite is needed in these materials.Whereas for series with 2% graphite content (S2 and SZ2), sample with only zircon as abrasive (SZ2) has higher wear resistance, series with 4% graphite (S4 and S4Z) do not show this tendency. In this case, it is S4 what presents the highest wear resistance.

3.3.2. *As function of graphite's type*

To study the influence of graphite's type, i.e. natural (flaky morphology) vs. synthetic (granular morphology), on processing and properties of friction materials, a new composition named S4N (4 wt. % natural graphite) was prepared (Table 2). As shown in Table 1, the average particle size of natural and synthetic graphite is 300 μm and 21 μm, respectively.

The samples were prepared following both processing routes. However, in Route 2 samples were not cold pressed after sintering stage because natural graphite particles were not well embedded and bonded in the bronze matrix and they came off during manipulation of as-sintered preforms, as shown in Fig. 15. This is related to the fact that when powder blend was deposited in molds, natural graphite particles were floating, making sintering difficult by this route and obtaining samples very poorly sintered. This problem might be related with the graphite particle size and its morphology (flaky) since large graphite particles decreases, even more, the wettability of graphite by bronze.

Table 10 shows the apparent density and porosity of compositions S4 and S4N. Values for Route 2 are that obtained after sintering stage. Mechanical resistance only was measured in samples processed by Route 1. As observed in this table, material with natural graphite processed by Route 1 (S4N) achieves higher density than the material with synthetic one (S4). This might be because of the lower springback of natural graphite compared to the synthetic one, which takes place during sintering, since their green density are similar. This difference is really noticed in mechanical properties, which significantly increase when natural graphite is used. On the other hand, materials with natural graphite that were processed by Route 2 (S4N) achieve lower densification during sintering.

4. Conclusion

According to the results shown in this paper, liquid phase sintering is required to achieve good densification of bronze sintered matrix friction materials, but sintering temperature has to be lower than 900 °C to avoid excess of liquid, which would exude from the specimens. Samples processing by R1 and R2 were satisfactory sintered at 850 and 875 °C, respectively.

Regarding abrasives size, better properties, mainly tribological performance, are achieved using coarse abrasives (S series). Their low specific surface area makes densification during sintering easier and consequently bronze particles matrix are better bonded and abrasives are better embedded in the matrix, obtaining, thereby, materials with high mechanical resistance, stable friction coefficient and low wear. On the contrary, fine abrasives (F series) interfere more during sintering hindering the bonding and densification of the bronze metal matrix. Therefore, materials with fine abrasives present higher wear and unstable friction behavior.

The detrimental effect of fine abrasives in the sinterability and friction performance is even more noticeable in materials processed by R2, since in this route loose powder is more difficult to be sintered compared to the green compact used in R1.

Increasing graphite content leads to a reduction in physical and mechanical properties. Nevertheless, it improves the tribological behavior, since materials with 4% of synthetic graphite present better stability in friction coefficient and low wear, especially in samples produced by Route 2. By this route, natural graphite, due to its particular morphology, is not appropriate.

Declarations

Author contribution statement

J. Echeberria: Conceived and designed the experiments; Analyzed and interpreted the data.

B. Pérez Polo: Performed the experiments; Analyzed and interpreted the data; Wrote the paper.

Funding statement

This research did not receive any specific grant from funding agencies in the public, commercial, or not-for-profit sectors.

Competing interest statement

The authors declare no conflict of interest.

Additional information

No additional information is available for this paper.

References

[1] W. Schatt, K. Wieters, Powder Metallurgy. Processing and Materials, European Powder Metallurgy Association (EPMA), Shrewsbury, 1997.
[2] V. Jain, M. Saravanan, R.C. Anandani, R. Sikand, A.K. Gupta, Effect of sizing on friction and wear properties of copper-iron based sintered composites, Trans. Indian Inst. Met. 63 (1) (2010) 43–54.
[3] L. Su, F. Gao, X. Han, R. Fu, E. Zhang, Tribological behavior of copper-graphite powder third body on copper-based friction materials, Tribol. Lett. 60 (2) (2015) 1–12.
[4] M. Boz, A. Kurt, Effect of ZrSiO4 on the friction performance of automative brake friction materials, J. Mater. Sci. Technol. 23 (6) (2007) 843–850.

[5] R.L. Cox, Engineered Tribological Composites: the Art of Friction Material Development, SAE International, Warrendale, Pennsylvania, USA, 2012.
[6] X. Xiong, J. Chen, P. Yao, S. Li, B. Huang, Friction and wear behaviors and mechanisms of Fe and SiO2 in Cu-based P/M friction materials, Wear 262 (9–10) (2007) 1182–1186.
[7] G. Kwabena Gyimah, P. Huang, D. Chen, Dry sliding wear studies of copper-based powder metallurgy brake materials, J. Tribol. 136 (4) (2014).
[8] B. Chen, Q. Bi, J. Yang, Y. Xia, J. Hao, Tribological properties of solid lubricants (graphite, h-BN) for Cu-based P/M friction composites, Tribol. Int. 41 (12) (2008) 1145–1152.
[9] M. Boz, A. Kurt, The effect of Al2O3 on the friction performance of automotive brake friction materials, Tribol. Int. 40 (2007) 1161–1169.
[10] K.H. Cho, H. Jang, Y.S. Hong, S.J. Kim, R.H. Basch, J.W. Fash, The size effect of zircon particles on the friction characteristics of brake lining materials, Wear 264 (3–4) (2008) 291–297.
[11] E.J. Lee, H.J. Hwang, W.G. Lee, K.H. Cho, H. Jang, Morphology and toughness of abrasive particles and their effects on the friction and wear of friction materials: a case study with zircon and quartz, Tribol. Lett. 37 (3) (2010) 637–644.
[12] T. Ram Prabhu, V.K. Varma, S. Vedantam, Effect of reinforcement type, size, and volume fraction on the tribological behavior of Fe matrix composites at high sliding speed conditions, Wear 309 (1–2) (2014) 247–255.
[13] Y. Xiao, et al., Mechanical and tribological behaviors of copper metal matrix composites for brake pads used in high-speed trains, Tribol. Int. 119 (2018) 585–592.
[14] Y. Zhan, G. Zhang, Friction and wear behavior of copper matrix composites reinforced with SiC and graphite particles, Tribol. Lett. 17 (1) (2004) 91–98.
[15] P.T. Dewisme, Desarrollo de materiales de fricción basados en metal sinterizado para aplicaciones en frenos de la industrial eólica, Universidad de Navarra, Tecnun, 2014.
[16] A.M. Martinez, La sustitución del cobre en las pastillas de freno orgánicas mediante polvos metálicos y el estudio de su reacción con los lubricantes sólidos, Universidad de Navarra, Tecnun, 2015.
[17] L. Fuentes-Pacheco, M. Campos, Lead-free copper- base alloys for friction components: sinterability and recrystallization, Int. J. Powder Metall. 48 (3) (2012) 29–39.
[18] X. Xiao, Y. Yin, J. Bao, L. Lu, X. Feng, Review on the friction and wear of brake materials, Adv. Mech. Eng. 8 (5) (2016) 1–10.
[19] T.R. Prabhu, Effects of solid lubricants, load, and sliding speed on the tribological behavior of silica reinforced composites using design of experiments, Mater. Des. 77 (2015) 149–160.
[20] J. Chen, X. Xiong, P. Yao, E. Al, Effect of rubbed surface temperature on friction behaviour of iron based P/M friction materials, Powder Metall. Technol. 22 (4) (2004) 223–227.
[21] B. Perez Polo, Materiales de fricción de metal sinterizado base cobre: Influencia de sus constituyentes en el procesamiento y propiedades tribológicas, Universidad de Navarra, Tecnun, 2019.
[22] X.-M. Han, F. Gao, B.-Y. Song, R. Fu, Effect of friction speed on friction and wear performance of Cu-matrix friction materials, Tribology 29 (1) (2009) 89–96.
[23] T. Ram Prabhu, Effect of bimodal size particles reinforcement on the wear, friction and mechanical properties of brake composites, Tribol. Mater. Surf. Interfaces 10 (4) (2016) 163–171.
[24] J. Kováčik, Š. Emmer, J. Bielek, L. Keleši, Effect of composition on friction coefficient of Cu-graphite composites, Wear 265 (3–4) (2008) 417–421.
[25] S.F. Moustafa, S.A. El-Badry, A.M. Sanad, B. Kieback, Friction and wear of copper-graphite composites made with Cu-coated and uncoated graphite powders, Wear 253 (7–8) (2002) 699–710.
[26] D. Gultekin, M. Uysal, S. Aslan, M. Alaf, M.O. Guler, H. Akbulut, The effects of applied load on the coefficient of friction in Cu-MMC brake pad/Al-SiCp MMC brake disc system, Wear 270 (1–2) (2010) 73–82.
[27] H. Kato, M. Takama, Y. Iwai, K. Washida, Y. Sasaki, Wear and mechanical properties of sintered copper-tin composites containing graphite or molybdenum disulfide, Wear 255 (2003) 573–578.